DETECTION OF INTERNALLY BRUISED BLUEBERRIES USING HYPERSPECTRAL TRANSMITTANCE IMAGING

M. Zhang, C. Li, F. Takeda, F. Yang

ABSTRACT. *Internal bruise damage that occurs in blueberry fruit during harvest operations and postharvest handling lowers the overall quality and causes significant economic losses. The main goal of this study was to nondestructively detect internal bruises in blueberries after mechanical damage using hyperspectral transmittance imaging. A total of 600 hand-harvested blueberries were divided into 20 groups of four storage times (30 min, 3 h, 12 h, and 24 h), two storage temperatures (22°C and 4°C), and three treatments (stem bruise, equator bruise, and control). A near-infrared hyperspectral imaging system was used to acquire transmittance images from 970 to 1400 nm with 5 nm bandwidth. Images were acquired from three orientations (calyx-up, stem-up, and equator-up) for fruit in the control and stem bruise groups and from four orientations (calyx-up, stem-up, equator-up, and equator-down) in the equator bruise groups. Immediately after imaging, the fruit samples were sliced, and the sliced surfaces were photographed. The color images of sliced fruit were used as references. By comparing with the reference color images, the profiles of spatial and spectral intensities were evaluated to observe the effect of orientation and help extract regions of interest (ROIs) of bruised and healthy tissues. A support vector machine (SVM) classifier was trained and tested to classify pixels of bruised and healthy tissues. Classification maps were produced, and the bruise ratio was calculated to identify bruised blueberries (bruise ratio >25%). The average accuracy of blueberry identification was 94.5% with the stem-up orientation. The results indicate that detecting bruised blueberries as soon as 30 min after mechanical damage is feasible using hyperspectral transmittance imaging.*

Keywords. *Blueberry, Bruise detection, Classification, Hyperspectral imagery, Transmittance mode.*

Blueberries have become popular around the world due to their appealing flavor and high nutraceutical value (Mazza et al., 2002). The U.S. produced 262,539 tons of blueberries in 2014, which was 50% of total world production (FAOSTAT, 2014). More than half of U.S. production went to the fresh market, generating more than $630 million (NASS, 2014). Most blueberries intended to be consumed fresh are hand-picked and transported over long distances. During harvesting and packaging, berries can be bruised by hand and mechanical impact. Bruise damage accelerates fruit decay during transport and lowers overall quality (Opara and Pathare, 2014; Takeda et al., 2013). Furthermore, bruised blueberries are less attractive to customers due to their shriveled appearance and lack of firm texture (Dale et al., 1994). As a result, fruit bruising causes significant economic losses in the blueberry industry due to degraded quality and rejection by the consumer (Chiabrando et al., 2009; Opara and Pathare, 2014; Prusky, 2011). Therefore, it is important to distinguish bruised blueberries from non-bruised blueberries to remove low-quality fruit from the fresh blueberry supply chain.

Blueberry internal bruises are not visible to the human eye. Under current industry standards, blueberry bruises are detected by tactile feel of the whole fruit or sometimes by visually assessing tissue discoloration after slicing berries in half. When a blueberry is impacted, the cellular structure can be damaged, causing free water to be released from the cells. Immediately after the impact, the bruising is not easy to observe in whole blueberries nor in sliced blueberries. After 1 or 2 h, the bruised tissues become soft and start to turn brown (Brown et al., 1974; Burda et al., 1990), so the bruising becomes clearer, but the edge of the bruising is not obvious in sliced fruit. Therefore, it is difficult for workers to identify

Submitted for review in December 2016 as manuscript number ITSC 12197; approved for publication by the Information, Technology, Sensors, & Control Systems (ITSC) Technical Community of ASABE in September 2017. Presented at the 2016 ASABE Annual International Meeting as Paper No. 162460707.

This research received the ITSC Technical Community Meeting Paper Award. The ITSC Technical Community Meeting Paper Award was established in 1999 to encourage high-quality papers in conjunction with presentations at ASABE Annual International Meetings. A certificate and recognition are given for up to four of the top meeting papers presented at an ITSC-sponsored or co-sponsored technical session. Additionally, approximately the top 10% of the submitted papers are explicitly invited for submission to an ASABE journal.

The authors are **Mengyun Zhang, ASABE Member,** Doctoral Student, College of Mechanical and Electronic Engineering, Northwest Agriculture and Forestry University, Yangling, China; **Changying Li, ASABE Member,** Professor, Bio-Sensing and Instrumentation Laboratory, College of Engineering, University of Georgia, Athens, Georgia; **Fumiomi Takeda,** Research Horticulturist, USDA-ARS Appalachian Fruit Research Station, Kearneysville, West Virginia; **Fuzeng Yang,** Professor, College of Mechanical and Electronic Engineering, Northwest Agriculture and Forestry University, Yangling, China. **Corresponding authors:** Changying Li, 712 F Boyd Graduate Studies Building, University of Georgia, Athens, GA 30602 (phone: 706-542-4696; e-mail: cyli@uga.edu), and Fuzeng Yang, P.O. Box 16, Northwest Agriculture and Forestry University, 22 Xinong Road, Yangling, Shaanxi 712100, China (phone: +86-029-87092913; e-mail: yfz0701@163.com).

the bruised region and grade the blueberry. After one day, the bruised tissues are very soft and discoloration continues to develop, enabling an experienced worker to easily distinguish the bruising. The disadvantages of these inspection methods are that they are time-consuming and their accuracy declines after a few hours of continuously monitoring the fruit (Opara and Pathare, 2014). Additionally, they are not effective for identifying bruised blueberries in the early stage of bruising. In addition, quantifying bruise damage by slicing the fruit is destructive. To address these issues, reference charts have been developed to assist graders in determining the bruise grade based on standard bruising scores (Toivonen et al., 2007). However, this approach is still subjective and too time-consuming.

Firmness measurement techniques have been developed to speed up the inspection process for fruit quality evaluation and produce more accurate grades, including firmness/texture analyzers for blueberry (Slaughter and Rohrbach, 1985), acoustic impulse-response measuring for tomato fruit (Schotte et al., 1999), and resonance frequency-based methods for peach fruit (Goliáš et al., 2003). These methods can provide more accurate measurements of firmness, but many of the firmness measurement techniques require directly contacting the fruit and therefore could potentially cause damage to blueberries.

Visible/near-infrared (Vis/NIR) spectroscopy has been shown to have potential for detecting internal defects such as watercore, internal browning, internal breakdown, and insect infestation with rapid and nondestructive measurement. For example, Upchurch et al. (1997) identified apples with internal breakdown using body transmittance and achieved more than 85% accuracy in detecting defective apples. Clark et al. (2003) found that apple browning affected the spectral information and had stronger absorbance in the red area of the spectrum. Vis-NIR spectroscopy was also reported for detecting physiological disorders, such as water-soaked and browning flesh in melons (Ito et al., 2003), and for predicting storage disorders in kiwifruit (Clark et al., 2004). However, the limitation of conventional NIR spectroscopy is that a single spectrum collected from one area of the fruit may not be a good representation of the entire fruit.

In the past decade, hyperspectral imaging has emerged as a powerful technique that can provide both spectral and spatial information without contacting the samples. Hyperspectral imaging has been used to detect bruises and bitter pit in apples (Xing et al., 2007) (<3% misclassification of apple bruises) and chilling injuries in cucumbers (Cheng et al., 2004) (>80% accuracy) using the diffuse reflectance mode. To extend the application of this technology, the transmittance mode was developed to acquire hyperspectral images for food quality assessment. The transmittance mode, in which the fruit surface scanned by the detector is diametrically opposite to the illuminated surface (Kawano et al., 1993; Miyamoto and Kitano, 1995), may be less sensitive to surface properties and better for detecting internal quality than the reflectance mode (Schaare and Fraser, 2000). Qin and Lu (2005) used hyperspectral transmittance imaging combined with a neural network to detect pits in tart cherries and achieved low average classification errors (<3%). Cucumber samples that had internal damage displayed higher transmittance values than cucumber samples with no internal damage, and the transmittance mode achieved >90% accuracy in this classification (Ariana and Lu, 2008). The researchers also reported that the hyperspectral imaging system performed better than human inspection, and the transmittance mode achieved higher detection rates (88% to 93%) than the reflectance mode (82% to 88%) for pest infestation (Lu and Ariana, 2013).

More recently, Hu et al. (2016) used reflectance, transmittance, and interactance imaging spectroscopy to detect blueberry mechanical damage in the spectral range of 328 to 1113 nm. They reported that several transmittance-based classifiers obtained satisfactory accuracies (79.1% for logistic regression, 74.4% for multilayer perceptron with backpropagation, and 72.1% for logistic function tree) in classifying damaged blueberries 48 h after the blueberries were impacted, but the methods performed poorly for early detection (only 30% to 50% accuracy). Furthermore, Jiang et al. (2016) used hyperspectral imaging with the reflectance mode to detect bruising in blueberries at 24 and 48 h after the blueberries were impacted. Hyperspectral reflectance imaging in the spectral range of 950 to 1650 nm achieved excellent classification results (94%, 92%, and 96% for the training set, independent test set, and combined set, respectively). The limitation of that study was that the bruised part of the blueberry needed to face the camera. In a practical application, the bruised areas of blueberries may not be perfectly positioned to face the camera.

Packaging, storage, and temperature affect the rate of fruit deterioration. After packaging and during transportation, blueberries are held at low temperatures (0°C to 4°C). In general, low temperatures reduce bruise damage (Van linden et al., 2006), but it is still important to monitor the development of bruise damage at low temperatures (Opara and Pathare, 2014). Hu et al. (2016) reported that their classification accuracies for bruised blueberries evolved with time, but they did not perform their experiment at a low temperature.

Therefore, the overall goal of this study was to explore the possibility of early detection of blueberry internal bruise damage using hyperspectral transmittance imaging in the near-infrared spectral range within 24 h after impact at two storage temperatures (22°C and 4°C). The specific objectives were to: (1) inspect the transmittance spatial and spectral profile differences between bruised and healthy blueberries and the effects of fruit orientation to the imaging data, (2) investigate the development of bruise damage in blueberries over time at two temperatures, and (3) use the established classification model to classify the pixels of bruised and healthy tissues from various groups to explore the feasibility of early detection.

Materials and Methods

Sample Preparation

Mature fruit of the southern highbush blueberry (*Vaccinium corymbosum* hybrids) cultivar 'Farthing' were harvested by hand at a commercial farm in Alma, Georgia, in May 2016. The samples were manually selected so that all of the

Table 1. Sample size of each group with various treatments.

Storage Time	Impact Position[a]	Storage Temperature 22°C	4°C	Total
30 min	Stem End	30	30	60
	Equator	30	30	60
	None	30	30	60
3 h	Stem End	30	30	60
	Equator	30	30	60
12 h	Stem End	30	30	60
	Equator	30	30	60
24 h	Stem End	30	30	60
	Equator	30	30	60
	None	30	30	60
Total		300	300	600

[a] "None" = control groups (no impact on blueberries).

berries were of a similar size and blemish-free. The samples were packed into clamshells and then stored at 4°C in a refrigerator. The intact blueberries were separated into 20 groups of 30 fruit each (table 1). The control groups were kept intact, whereas the bruising treatments were applied using a pendulum (Yu et al., 2014) with an arm length of 30 cm to impact fruit against a steel plate either at the stem end or the equator (fig. 1). The total weight of the blueberry fixator and the wooden arm was 29.45 g. Blueberry bruising development was investigated at two temperatures: room temperature (22°C) and cold storage simulation (4°C). Before bruising treatments, the 22°C groups were taken out of the refrigerator and stored in an air-conditioned room for 2 h to let them warm to room temperature (22°C). The 4°C groups were briefly removed from the refrigerator during the bruising treatments and then quickly returned to the refrigerator to simulate impacts occurring at low temperature (4°C). After bruise creation and before acquiring images, the 22°C groups were stored in the air-conditioned room (at 22°C), and the 4°C groups were refrigerated (at 4°C) for 30 min, 3 h, 12 h, or 24 h, depending on the storage time to which the group was assigned. The four control groups were stored at 22°C for 30 min, at 22°C for 24 h, at 4°C for 30 min, and at 4°C for 24 h before imaging. An intact blueberry does not change much within 24 h in terms of weight loss, water loss, or tissue decay (Almenar et al., 2008; Jackson et al., 1999), so there were no control groups for the storage times of 3 and 12 h. After treatment, all groups were kept enclosed in plastic wrap before image acquisition.

Acquisition of Hyperspectral and Reference Images

A near-infrared hyperspectral imaging system (Wang et al., 2012) was used to acquire transmittance images of blueberry fruit placed on a black sample holder that had an 8 mm diameter hole (fig. 2). To provide uniform lighting, a 12 V,

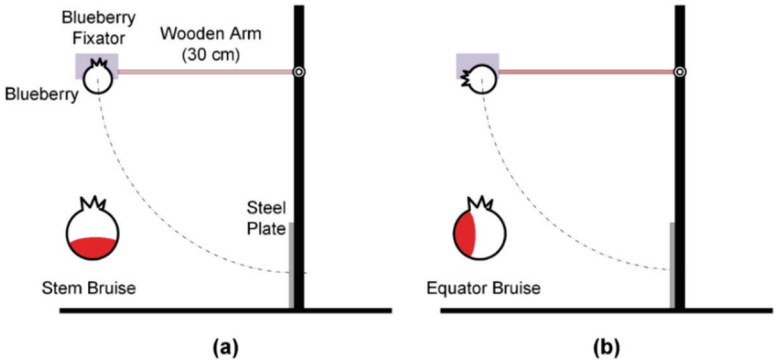

Figure 1. Pendulum apparatus used to create blueberry bruises and positions of the bruises (shaded area on the fruit).

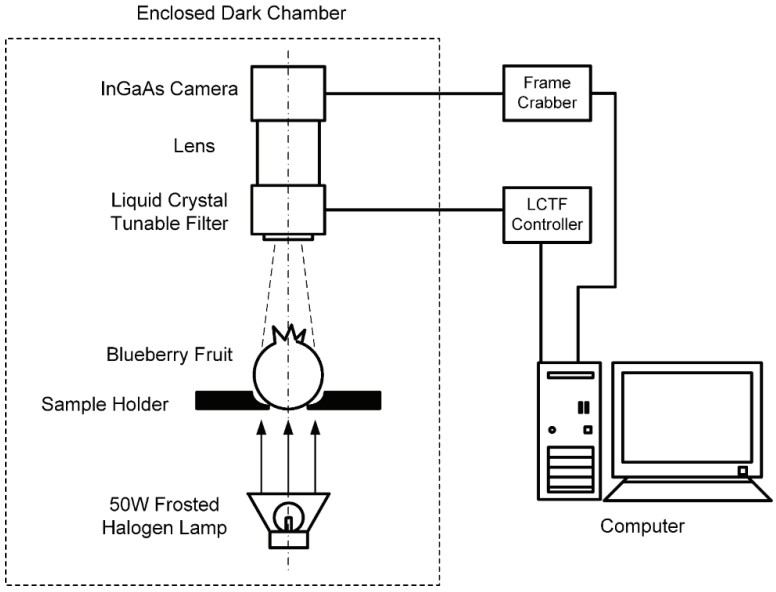

Figure 2. Schematic of hyperspectral transmittance imaging system.

50 W frosted halogen lamp with a smooth beam pattern that eliminated hot spots and shadows was installed below the sample holder. The distance between the sample holder and the lamp was 15 cm, and the distance between the filter of the image system and the sample holder was 87.5 cm. A dark chamber was used to enclose the system when acquiring images to exclude interference from ambient light. The nominal spectral response range of the imaging system was 850 to 1850 nm. In this study, hyperspectral transmittance images were acquired from 970 to 1650 nm, at 5 nm spectral intervals, because of the low signal-to-noise ratios at the beginning and end of the spectrum.

To investigate the effects of fruit orientation, three different orientations (calyx-up, stem-up, and equator-up) of blueberries in the control groups and stem bruise treatment groups were used when acquiring images of each blueberry (fig. 3). For the equator bruise treatment, in addition to the calyx-up and stem-up orientations, equator-up orientation (bruised area facing toward the camera) and equator-down orientation (bruised area facing away from the camera) were investigated, making four orientations for this treatment. Prior to collecting fruit images, a white reference image was acquired from a polytetrafluoroethylene (PTFE) Teflon plate (20 mm thickness), and a dark reference image was acquired by covering the filter of the imaging system. White and dark reference images were acquired again after every 18 images.

After image acquisition, all samples were cut into halves along the bruised position, and the cross-sections of the sliced fruit were imaged with a digital camera (Lumix G6, Panasonic, Osaka, Japan) under room illumination to serve as RGB reference images for internal bruising evaluations.

Spatial and Spectral Information Extraction

The acquired hyperspectral transmittance images were calibrated using a flat-field correction algorithm implemented in Interactive Dynamic Language (IDL4.7, Exelis Visual Information Solutions, Boulder, Colo.) (Wang et al., 2012) using the white and dark reference images. Based on a preliminary test, the intensities of the transmittance spectrum were very close to zero in the range of 1450-1650 nm, so the spectral range was truncated to 970-1400 nm (87 wavelength bands). The image of each blueberry was cropped to 55 × 55 pixels to remove the noise around the border.

Transmittance spatial and spectral intensity profiles were extracted from the hyperspectral images of the stem bruise group, the equator bruise group, and the control group at storage temperature of 22°C and storage time of 24 h because the browning of bruises on the blueberries at the high temperature with longer storage time was most pronounced at the image level (Jiang et al., 2016). The profiles were used to investigate the spectral information of healthy and bruised tissues and to inspect the effect of different orientations of berries in bruise detection.

To observe the effects of different storage times and temperatures, one blueberry was randomly picked from each of the 20 groups, and the blueberries were displayed in the form of a grayscale image extracted from the hyperspectral transmittance image. These 20 blueberries were then sliced in half, and color (RGB) images of the blueberry slices were taken with a DSLR camera for use as reference images to assist in manually selecting the regions of interest (ROIs) in the hyperspectral transmittance images. The spectral information was extracted from the ROIs of each treatment group.

The RGB images of the blueberry slices were used to manually calculate the bruise ratio by counting the number of pixels in bruised or discolored tissues and the number of pixels in the whole cross-section, and then dividing the bruised and discolored pixel count by the whole cross-section pixel count to provide ground truth information. Analysis of variance (ANOVA) was performed to investigate the differences in fruit bruising between various treatments using SAS (ver. 9.3, SAS Institute, Inc., Cary, N.C.), and ENVI (ver. 4.7, ITT Visual Information Solutions, Boulder, Colo.) was used to conduct profile extraction, ROI extraction, and manual bruise ratio generation.

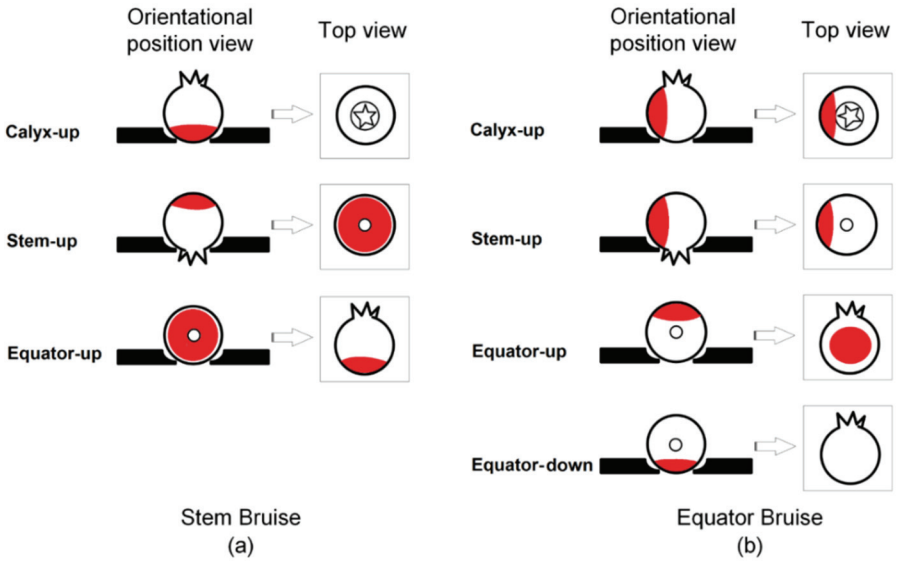

Figure 3. Orientations used for acquiring images of blueberry fruit: (a) three orientations (calyx-up, stem-up, and equator-up) used for the control and stem bruise groups and (b) four orientations (calyx-up, stem-up, equator-up, and equator-down) used for the equator bruise groups. The shaded area on the fruit indicates the bruised part.

Classification Method

The transmittance spectra of pixels extracted from ROIs were used as the training set. Every spectrum of each pixel was treated as an observation, and each wavelength was used as a variable (87 variables). A support vector machine (SVM) was used to classify pixels as either bruised or healthy tissue. In this study, the fine Gaussian function was selected as the kernel function. The kernel scale was 2.3, and the box constraint level was 1. The training set was used to train the SVM classifier, and the classifier was evaluated by four-fold cross-validation.

To verify the capability of the SVM classifier and explore the early detection of bruises, the SVM classifier was applied to all the pixels (beyond the ROIs) in the hyperspectral images. Thirty images of berries in the same group were mosaicked at each wavelength to form a new hyperspectral image cube containing 30 berries to conduct classification. The grayscale image was used to produce a mask to segregate blueberries from the background and remove the noise around the blueberries. The mask was generated using thresholding and morphological reconstruction. First, according to a previous study (Zhang and Li, 2016), the grayscale image at 1070 nm was thresholded by an intensity value of 3000. Next, morphological reconstruction was used to fill holes and remove noise pixels, and the refined image was used as the mask. Additionally, individual blueberries were recognized by calculating connected regions in the mask. The mask was applied to the hyperspectral images at the full range of wavelengths. Finally, the trained SVM classifier was used to classify each pixel of each blueberry in the masked hyperspectral images.

After classification, a classification map of the results was generated for every group. The pixels of the bruised areas and of the entire visible surface of the fruit were counted. Afterward, the bruise ratio was derived by dividing the pixel count of bruised tissue regions by the whole fruit pixel count. After bruise ratio calculation, the individual blueberries were identified as bruised if their bruise ratio exceeded 25%. Yu et al. (2014) and Hu et al. (2016) defined bruising as >25% of the cross-sectional area. Brown et al. (1996) indicated that blueberry firmness would decline significantly during storage in samples with bruise damage on >25% of the cut surface area. Classifier training, mask generation, classification map generation, and bruise ratio calculation were executed in MATLAB (ver. 2016a, The MathWorks, Inc., Natick, Mass.).

Results and Discussion

Spectral and Spatial Profiles

For the control group at 22°C after 24 h, the horizontal and vertical spatial profiles at 1070 nm were not different at any orientation (fig. 4). However, the intensities were higher for the edges than for the center tissues. These areas were bright, probably because of their shorter optical path or the decaying tissues, and they could be mistakenly classified as bruised tissues, which would be a false positive. For the calyx-up orientation, the spatial intensities were higher for the calyx core than for other tissues in the pixel range of 20 to 35, which is also visible in the grayscale image at 1070 nm. The same trend was present in the spectral profiles in the 970-1150 nm range. In early detection of bruises, it was difficult to distinguish the calyx core as bruised tissue or healthy tissue. Further experiments should be designed to explore this phenomenon by investigating the optical properties of the calyx. For the stem-up orientation, there were only minor differences between the spectral profiles of the two selected pixels. For the equator-up orientation, the spectral profiles were similar to those of stem-up. The average intensity with the equator-up orientation was slightly lower than with the stem-up orientation, likely due to the spheroid shape of blueberry fruit (i.e., the diameter at the equator is greater than the length of the stem-calyx axis). Using the RGB images as references, the tissue of the control group had light color and few bruises in the cross-section.

In the stem bruise treatment at 22°C after 24 h, the profiles of the groups with bruise treatments had distinct features compared with the control group (fig. 5). The stem-bruised samples showed an overall higher intensity in the spatial and spectral profiles than the control group. The higher intensity of bruises detected by the transmittance mode was also reported for pears (Han et al., 2006) and pickling cucumbers (Ariana and Lu, 2008). This could be because the bruised tissues leaked water from the cells, became loose, and collapsed. Bruised cells were observed to burst and detach in 'Golden Delicious' apples under scanning electron microscopy (SEM) (Mitsuhashi-Gonzalez et al., 2010). Cell membrane damage that led to leakage could account for increased light transmission in blueberry bruises. The abilities of cellular components (e.g., cell wall, membrane, and starch) to scatter light, generally in the form of diffracted or reflected light, might have decreased because the ruptured cells caused fluid leakage buildup (Ariana and Lu, 2008; Lu et al., 2010; Miller et al., 1995). When the refractive index of the cell walls coordinates with that of the infiltrating liquid, reflectance approaches a minimum and transmission approaches a maximum (Vogelmann, 1993); therefore, the blueberry bruises were observed as darker pixels using the reflectance mode (Jiang et al., 2016). In this study, using the transmittance mode, bruised areas were observed as bright pixels in the near-infrared spectral range.

The orientations also had effects on the images. As previously discussed, calyx-up was not an ideal orientation for detection of bruises because of interference from the calyx. For the stem-up orientation, the average intensity of the bruised tissue was higher than for the control group, but no distinct differences between spatial profiles were observed. For the equator-up orientation, the bruised tissues in the stem area presented higher intensities in both the spatial and spectral profiles. The spectral contrast between bruised and healthy tissues was greatest at about 1070 nm. The bruised tissues appeared much darker than healthy tissues in the RGB images of the sliced fruit.

Bruised tissues of blueberries in the equator bruise treatment groups were also expressed clearly in the spatial and spectral information for the calyx-up and stem-up orientations (fig. 6). The intensity of the spatial and spectral profiles on the bruised side was significantly higher than for healthy tissue. For the equator-up and equator-down orientations, the

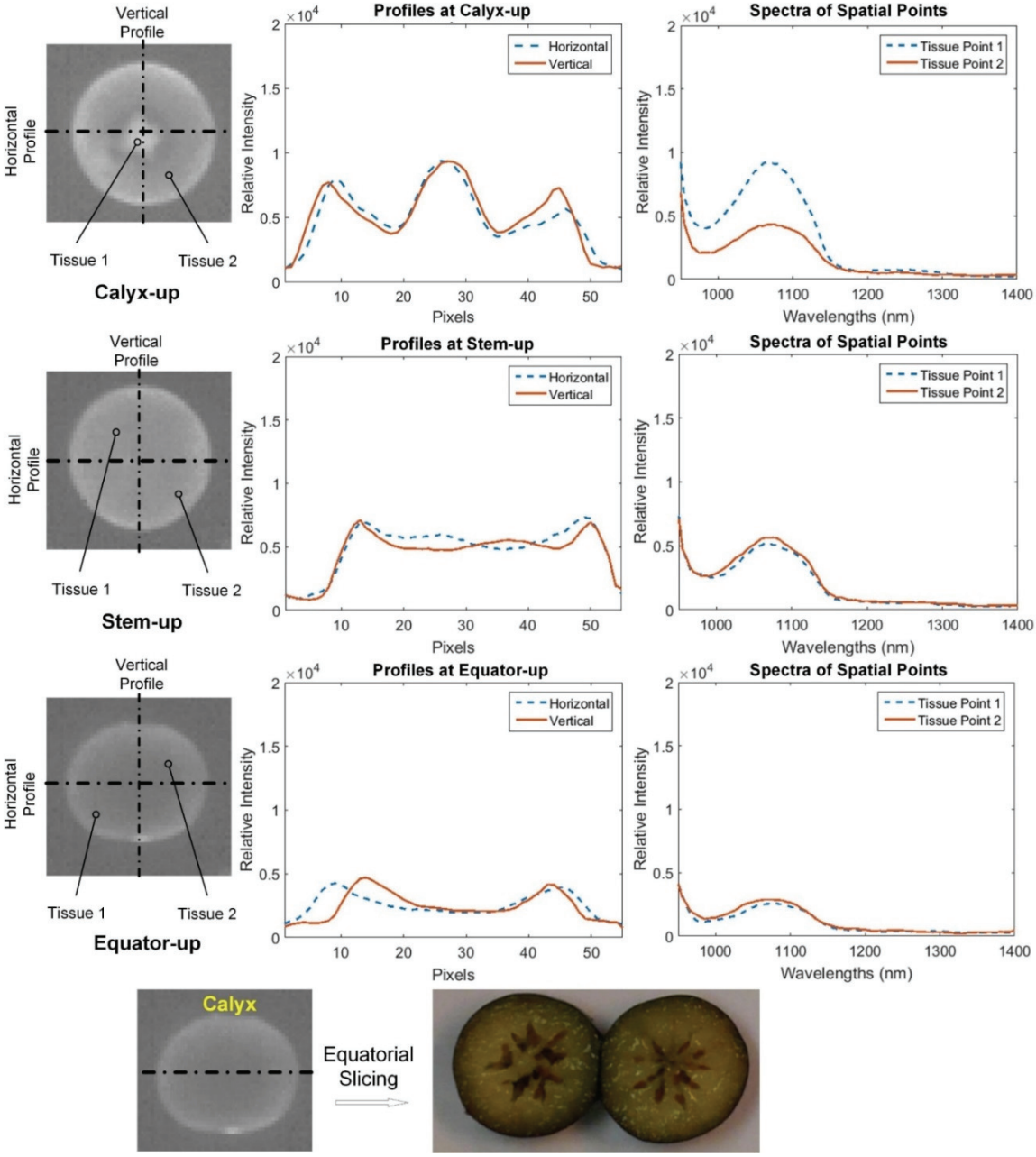

Figure 4. Three grayscale images (55 × 55 pixels) at 1070 nm of one fruit from the control group at 22°C after 24 h in three orientations (left), vertical and horizontal profiles of the three orientations at 1070 nm (middle), spectral profiles at specified points in the images (right), and fruit slicing method and RGB reference image (bottom). Calyx-up, stem-up, and equator-up refer to the orientations shown in figure 3a.

intensities of the spatial and spectral profiles were not distinct for healthy and bruised tissues because the light passed through both healthy and bruised tissues.

Based on the spatial and spectral profiles from the three treatments with the various orientations, bruised tissues had higher transmittance intensities than healthy tissues. Calyx-up was not suitable for bruise detection because the intensities were higher in the calyx region than in healthy tissue. Thus, the pixels of healthy tissues in the calyx region might be misclassified as bruised tissues. The equator-up orientation might be effective for stem bruise detection, but it is not practical to orient blueberries this way in commercial processing. To apply this technology for bruise detection in commercial packing lines, further improvement is necessary to orient all fruit with their equators oriented toward the light source. Therefore, the stem-up orientation was chosen for further analysis of the hyperspectral images of all treatment groups.

Spectral Images at Various Storage Times and Temperatures

In comparison to the control groups, the bruised blueberries appeared with bright pixels in the transmittance spectral images (fig. 7). The best contrast between bruised and healthy tissues was obtained at 1070 nm. This pattern held true at both temperatures. For instance, in the stem bruise group at 22°C, bruising was visible at 30 min as bright pixels, and the pixels in the bruised areas looked increasingly

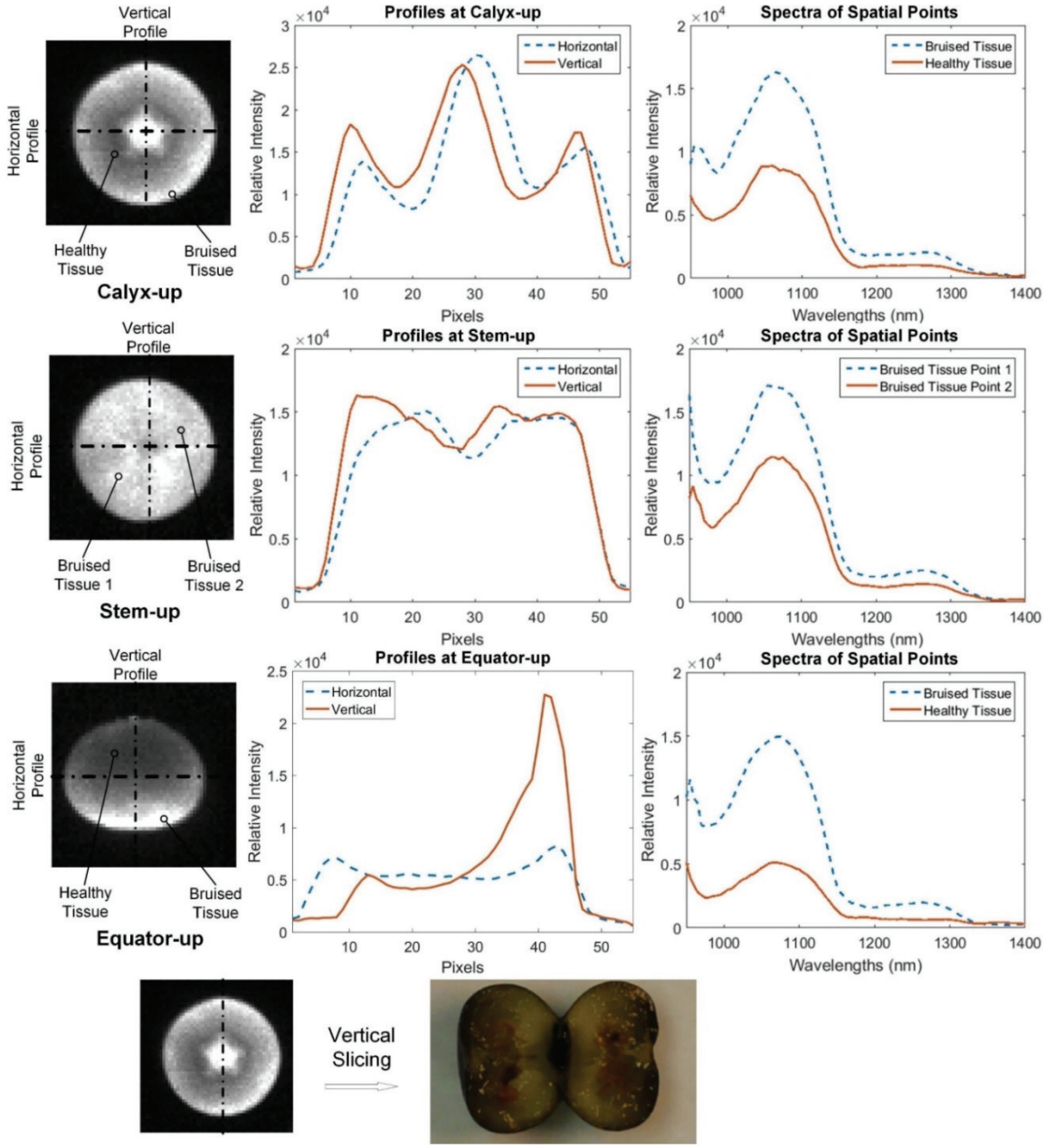

Figure 5. Three grayscale images at 1070 nm of one fruit from the stem bruise treatment group at 22°C after 24 h in three orientations (left), vertical and horizontal profiles of the three orientations at 1070 nm (middle), spectral profiles at specified points in the images (right), and fruit slicing method and RGB reference image (bottom). Calyx-up, stem-up, and equator-up refer to the orientations shown in figure 3a.

bright with increasing storage time (from 3 to 24 h). In the RGB reference images, the bruised tissues turned increasingly brown with time. At the lower temperature (4°C), the bruising (i.e., discoloration) did not develop as quickly as in the fruit stored at 22°C, but the bruise development followed the same trend.

For the equator bruise group at 22°C, the bruising developed over time, and the contrast between bruised and healthy tissues was clearly seen at 3 h in the grayscale images. At 4°C, bruises began to develop after 30 min of storage; the contrast between bruised and healthy tissues became clearer at 24 h. The ROIs were applied to the hyperspectral images of the stem-up orientation of bruised and healthy blueberry tissues.

Mean Spectra and Analysis of Bruise Development

The intensities of bruised tissues were considerably higher than those of healthy tissues for all groups in the spectral range of 1000 to 1120 nm (fig. 8). At both temperatures, the intensities of the bruised tissues increased over 24 h, and the equator bruise groups had relatively higher intensities than the stem bruise groups.

At 22°C, the difference in intensities between bruised tissues and healthy tissues was manifested at all storage times. The intensities of bruised tissues increased as bruising developed. For the stem bruise treatment, the spectra increased steadily with storage time. In contrast, the spectra of the equator bruise treatment reached a high level at 3 h and then

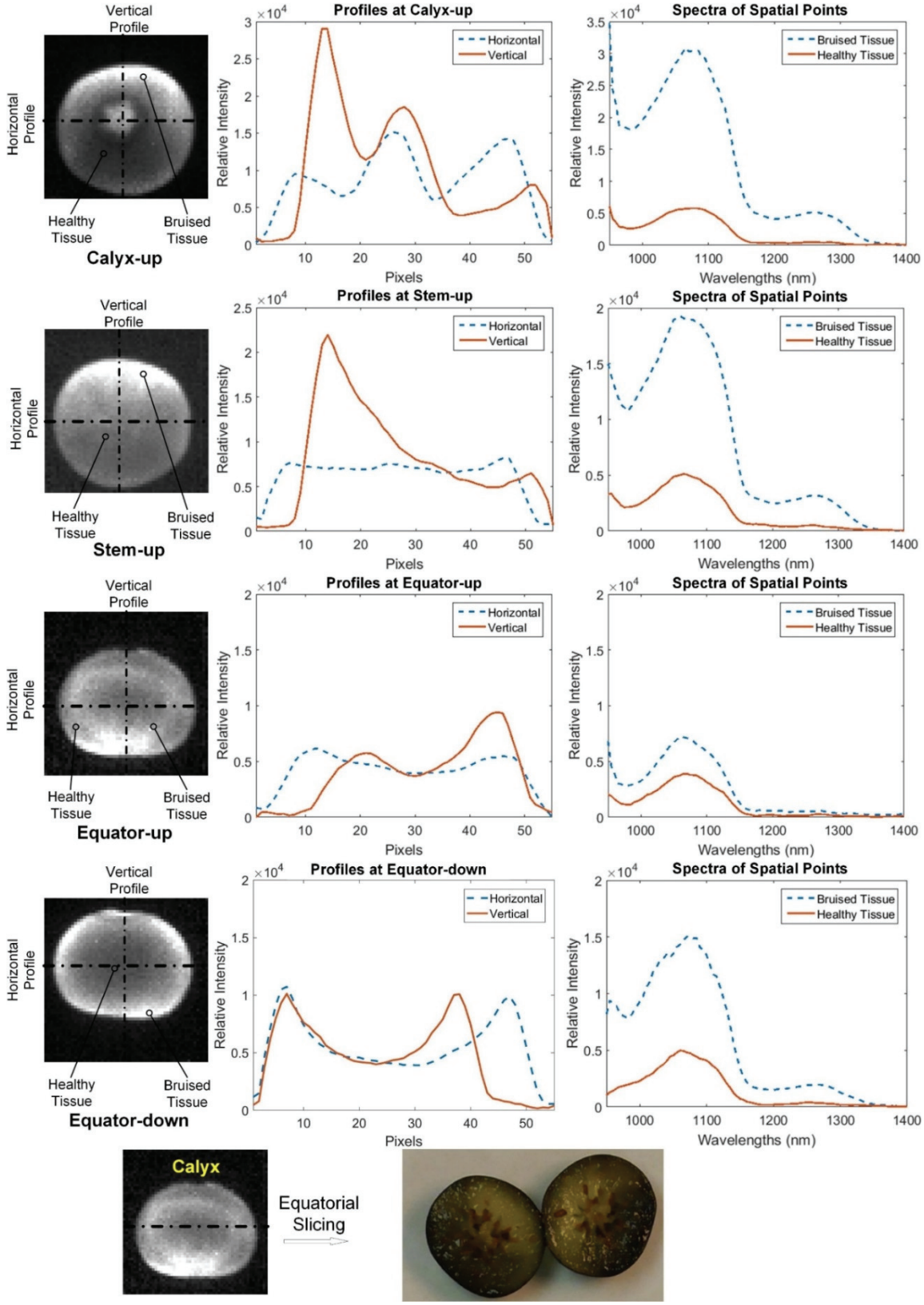

Figure 6. Four grayscale images at 1070 nm of one fruit from the equatorial bruise treatment group at 22°C after 24 h in four orientations (left), vertical and horizontal profiles of the four orientations at 1070 nm (middle), spectral profiles at specified points in the images (right), and fruit slicing and RGB reference image (bottom). Calyx-up, stem-up, equator-up, and equator-down refer to the orientations shown in figure 3b.

increased slowly. Very little difference was observed between the spectra of control groups at 30 min and 24 h; the spectra at 24 h was marginally higher, implying that the blueberry fruit was perhaps slowly deteriorating at room

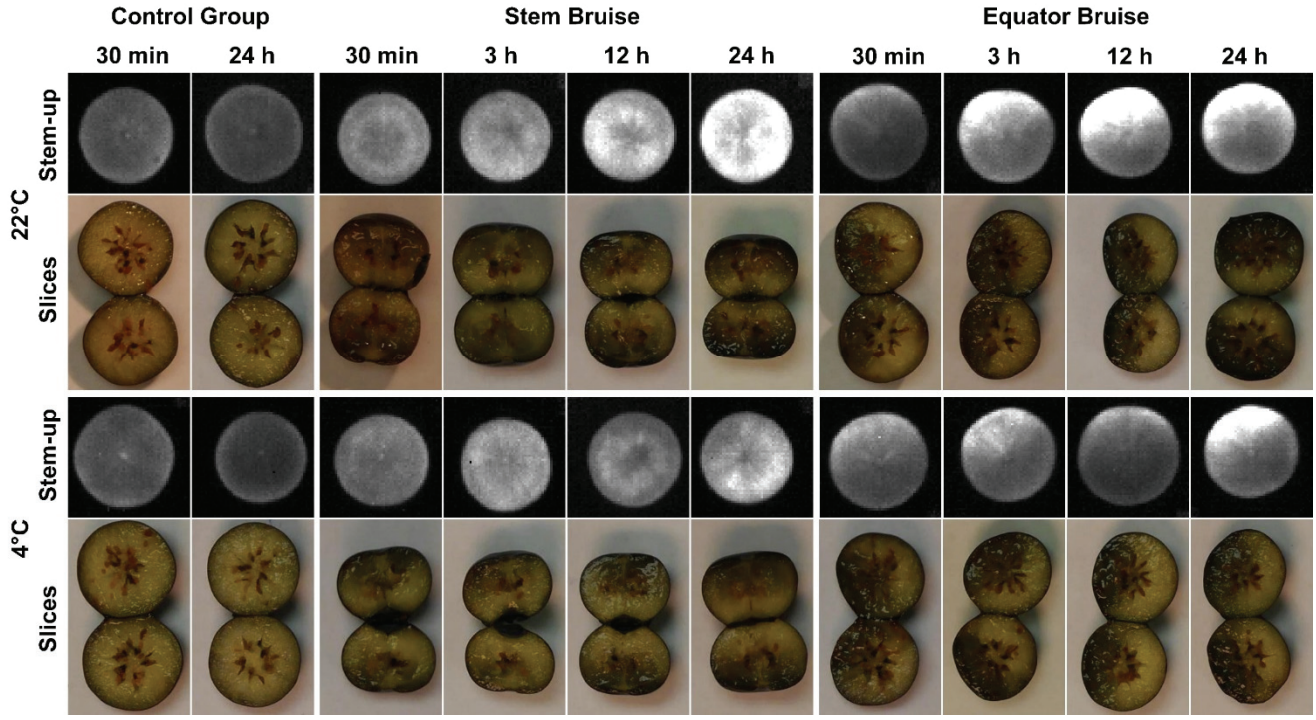

Figure 7. Spectral images (at 1070 nm with stem-up orientation) of one sample from each treatment group with two (for control) and four (for bruised) storage durations at 22°C and 4°C. RGB images of the sliced fruit (below the spectral images) provide references to internal bruising.

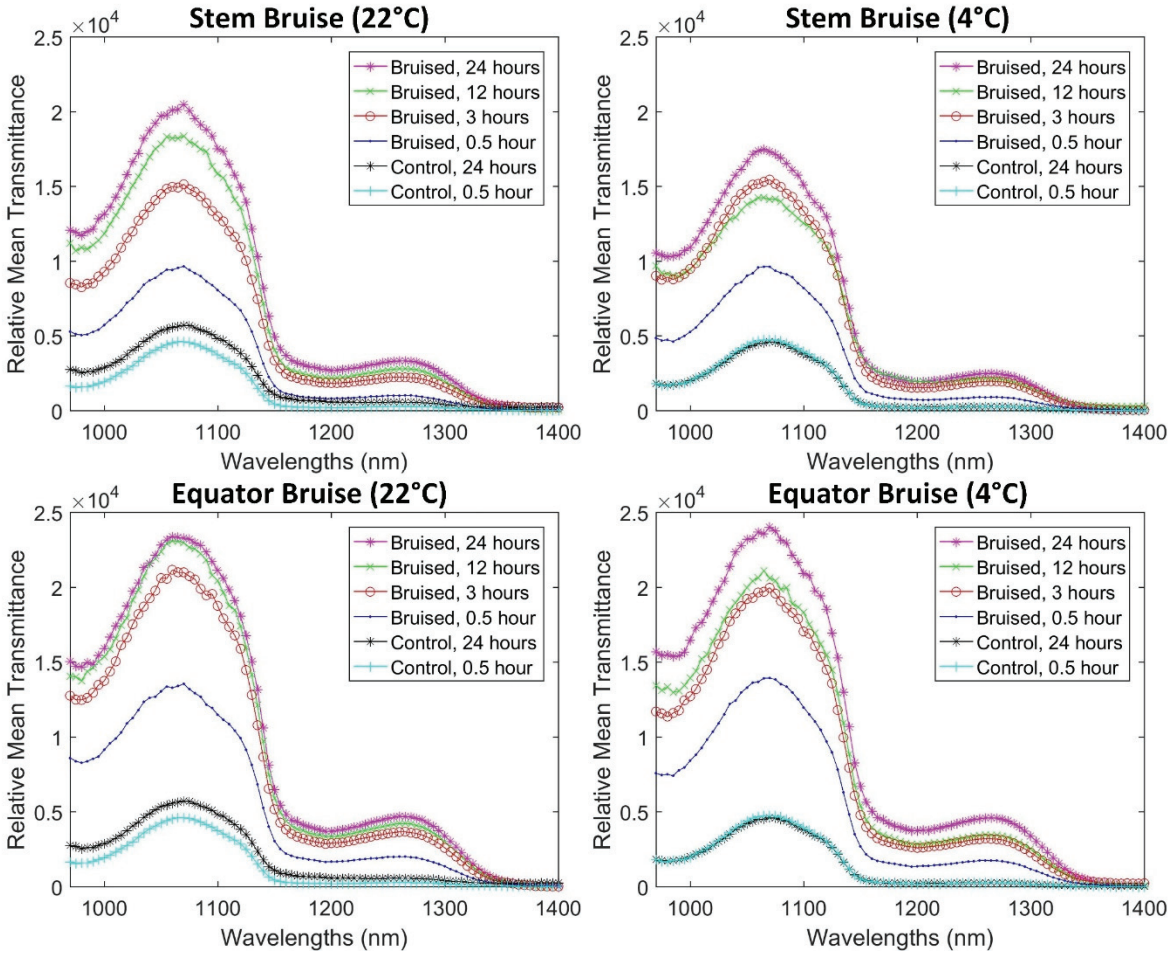

Figure 8. Mean spectra from healthy and bruised tissues 30 min, 3 h, 12 h, and 24 h after impact with stem-up orientation at 22°C and 4°C.

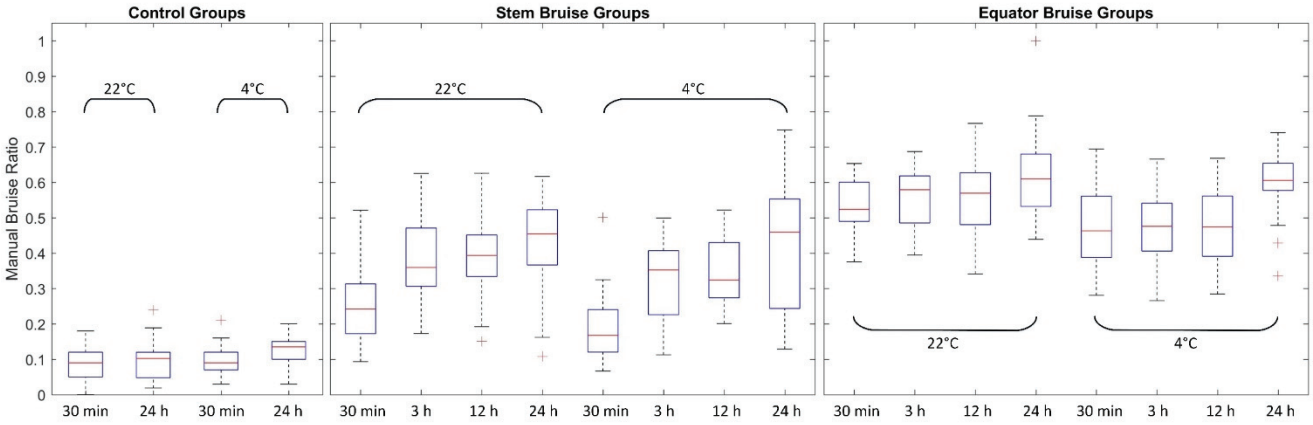

Figure 9. Comparison of manual bruise ratios for all 20 groups.

temperature.

At 4°C, the overall intensity of the stem bruise treatment was a bit lower than at 22°C, but the contrast between bruised and healthy tissues was still apparent. The spectral development trend of the equator bruise treatment was slower and finally reached the same high level as the high-temperature treatment at 24 h. There was little spectral difference between the control groups at 30 min and 24 h.

Regarding the grayscale images and mean spectra information, storage temperature usually affected tissue response to mechanical damage. Baritelle and Hyde (2001) showed that a higher handling temperature for both potatoes and pears correlated with a higher possibility of strain failure of the tissue. Temperature can influence a tissue's resistance to bruising by affecting the cell turgor; an increase in relative turgor reduces strain failure of the tissue. Higher temperatures can also provoke faster release of ethylene and CO_2, especially after an impact injury (DeMartino et al., 2002) of the blueberry. This is a result of autocatalytic ethylene production and is also responsible for the acceleration of apricot ripening (Nanos et al., 1997). An increase in the incidence of bruising with increasing storage time was also likely due to the respiration effect (Chiabrando et al., 2009; Nunes et al., 2004).

The results of the manual bruise ratios (fig. 9) and the statistical tests of the manual rating (table 2) matched the spectral information. The mean value of manual bruise ratios for the control group was considerably lower than that of the bruise treatments. Bruising developed further with longer storage time at both temperatures. The manual bruise ratio of the equator bruise treatment was relatively higher than that of the stem bruise treatment. This might be because the equator side of a blueberry is typically less firm than the calyx and stem ends, and softer tissues are more easily bruised (Tetteh, 2002).

Table 2. Duncan's multiple range test for manual bruise ratio.

		Mean Value	Duncan Grouping[a]
Treatment	Control	0.10	C
	Stem bruise	0.34	B
	Equator bruise	0.54	A
Storage temperature	22°C	0.39	A
	4°C	0.35	B
Bruise: Time effects[b]	30 min	0.36	C
	3 h	0.43	B
	12 h	0.44	B
	24 h	0.52	A
Control: Time effects[c]	30 min	0.09	B
	24 h	0.12	A

[a] Different letters indicate significant differences ($p < 0.05$).
[b] All bruise groups were combined.
[c] All control groups were combined.

PIXEL CLASSIFICATION

The overall accuracy was 99.65% when the pixels from the ROIs were used for classification (table 3). The occurrences of false positives and false negatives were low. This indicates that the spectra of healthy tissues and bruised tissues showed robust differences from each other. Jiang et al. (2016) achieved 96.25% accuracy in separating pixels of bruised and healthy tissues using reflectance mode. However, in that study, various cultivars of blueberries, including southern highbush cultivars ('Camellia', 'Rebel', and 'Star') and northern highbush cultivars ('Bluecrop', 'Jersey', and 'Liberty'), were used to extract the spectra. In this study, only one cultivar ('Farthing') was used, creating less natural variation. Thus, we expected our accuracy to be higher.

After applying the SVM classier to the hyperspectral images (including pixels beyond the ROIs), bruising was detected at the earliest time (30 min) at both 22°C and 4°C (fig. 10). This suggests that bruised blueberries can be detected at harvest and in processing lines using the transmittance imaging method. In the control groups, the borders of some blueberries were classified as bruised tissues. One reason for this false positive classification could be that the borders of some blueberries in the control groups were water-soaked tissues that were naturally decaying during transport and storage (Marlow and Loescher, 1984) but not yet browning. Another possible reason was that the flesh at the borders of blueberries is thinner than the center flesh, resulting in a shorter optical path. The intensities at the borders were higher and could be misclassified as bruised tissues. One way to avoid or minimize this phenomenon is to design a

Table 3. Confusion matrix of four-fold cross-validation of SVM classifier using data from ROIs (average accuracy = 99.65%).

	Predicted Healthy	Predicted Bruised	Total
True healthy	42,079 pixels (99.6% true negative)	170 pixels (0.4% false positive)	42,249
True bruised	139 pixels (0.3% false negative)	42,170 pixels (99.7% true positive)	42,309

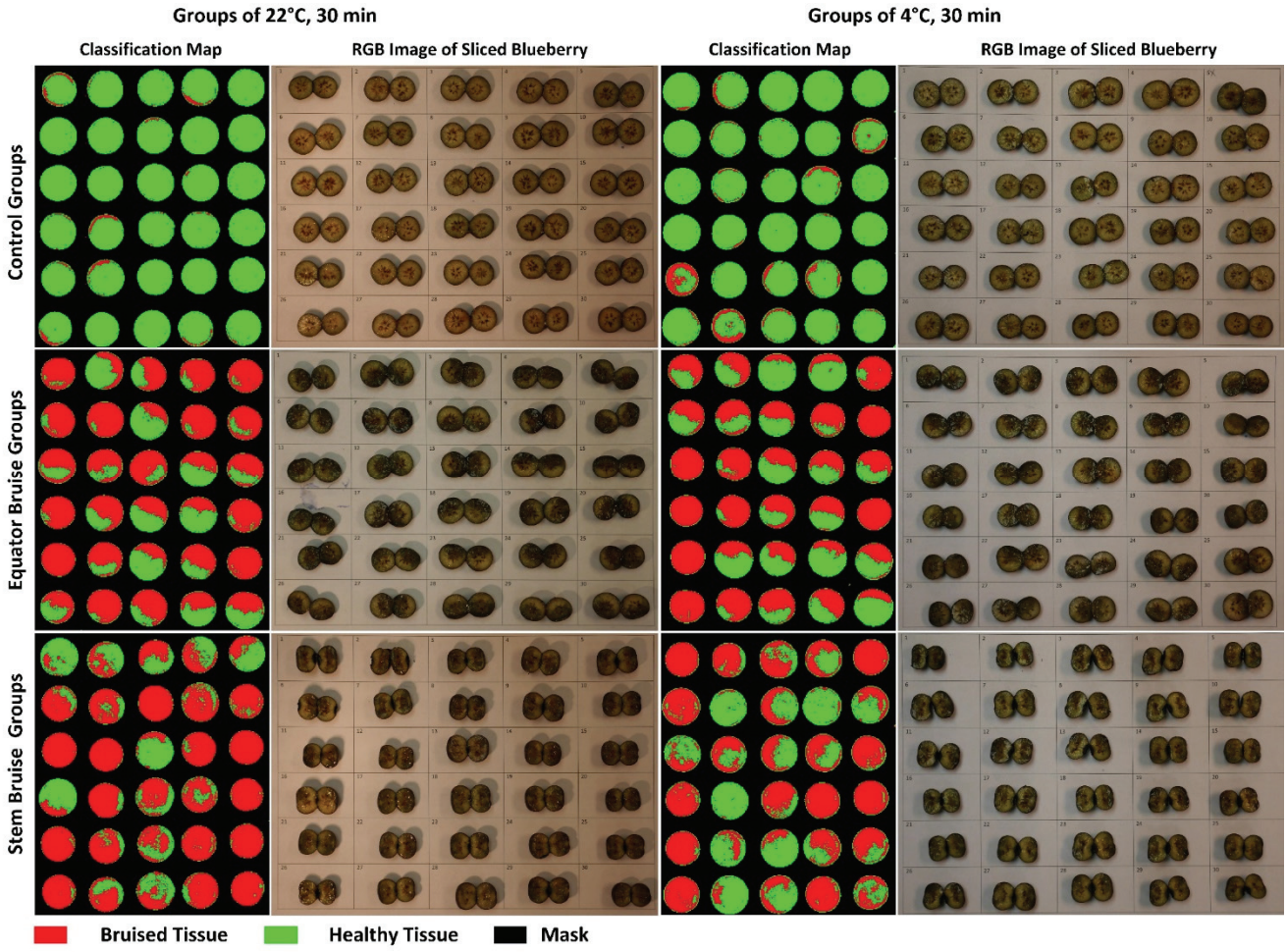

Figure 10. Classification maps and RGB reference images of control groups, stem bruise groups, and equator bruise groups with stem-up orientation 30 min after impact at 22°C and 4°C (six groups in total).

sample holder made of semitransparent material (e.g., Teflon plate) that compensates for the shape of the fruit so that the transmittance on the surface of the fruit is uniform. The material could also be heat resistant to mitigate the heating effect on the fruit.

When a 25% bruise ratio was set as the threshold to differentiate bruised or healthy fruit, the average SVM classification accuracy of healthy and bruised fruit for all treatment groups was 94.5% (table 4). The mean accuracies for 30 min were 96.7% at 22°C and 88.9% at 4°C. The results showed that bruises could be detected 30 min after impact, even at the low storage temperature of 4°C, which implied that the thresholding of 25% bruise ratio is efficient for the identification of healthy and bruised blueberries. At 22°C, the accuracies for the bruise treatments were greater than 90%. The accuracy of 86.67% was for the 24 h storage time for the control group. As discussed above, a few blueberries were misclassified because of the short optical path at the borders, or due to water-soaked tissues, or a combination of both. At 4°C, more bruised blueberries were misclassified as healthy berries due to the lower temperature, especially for groups imaged after 30 min. Misclassification also appeared in the stem bruise treatment because photons traveled through both healthy and bruised tissues with the stem-up orientation, and the differentiation power was reduced due to the mixed signals.

Table 4. Accuracies for distinguishing bruised and healthy blueberries by bruise ratio using SVM classifier (average accuracy = 94.5%).[a]

		30 min		3 h		12 h		24 h	
Storage Temperature	Bruise Treatment	Predicted	Accuracy (%)	Predicted	Accuracy (%)	Predicted	Accuracy (%)	Predicted	Accuracy (%)
22°C	Stem	27	90	27	90	30	100	29	96.67
	Equator	30	100	30	100	30	100	30	100
	Control	30	100	-	-	-	-	26	86.67
4°C	Stem	25	83.33	27	90	24	80	28	93.33
	Equator	27	90	30	100	30	100	30	100
	Control	28	93.33	-	-	-	-	29	96.67

[a] "Predicted" is the number of blueberries that were identified correctly using bruise ratio. A blueberry was classified as bruised if its bruise ratio was greater than 25%. There were 30 blueberries in each group. There were no storage treatments at 3 h and 12 h for the control group.

The SVM model showed overall high accuracies for predicting bruised and healthy blueberries at an early stage of damage using only the stem-up orientation. A prior study (Hu et al., 2016) achieved accuracies of approximately 75% and 90% for classifying damaged and intact blueberries, respectively, two days after impact using the mean transmittance spectra of whole blueberries. In our study, the locations of bruising were identified using spectra-based pixel classification. This method would be useful for researchers to evaluate the sensitivity of blueberries to mechanical damage, to interpret the bruising level, and to obtain more information about the bruising. Furthermore, this method has great potential for commercial application. The transmittance system could be implemented on a packing line to sort out internally bruised blueberries continuously and non-destructively. Compared to manual sorting, this method is non-contact and would not cause any damage during postharvest operations. However, more studies are needed to develop this technique for commercial use.

CONCLUSION

Bruised tissues of blueberries had higher transmittance intensities than healthy tissues in the spectral range of 1000 to 1150 nm. The largest difference between the spectral intensities of bruised and healthy tissues was at around 1070 nm. As bruising developed over time, the spectral intensities of the bruised tissues increased. Low temperature can slow bruising damage, but the spectral response pattern of bruised tissues in fruit stored at 4°C was similar to that of fruit held at 22°C. Based on the classification results of samples imaged using the stem-up orientation, it was feasible to detect bruises in blueberry fruit within 30 min after a mechanical impact whether the fruit were stored at room temperature or refrigerated. This study demonstrated the possibility of detecting bruised berries right after harvest in the field on a mechanical blueberry harvesting machine.

Additional experiments will be conducted to obtain the optical properties of bruised and healthy tissues of blueberries in the near-infrared spectral range and, in particular, to explore the influence of the calyx on the spectral response. Further analyses of feature selection and classifier optimization will be conducted to improve the efficiency and accuracy and to explore the capability of online bruise detection using hyperspectral imaging in transmittance mode. The technology presented in this article can improve automated machine sorting for separating bruised from non-bruised blueberries. In addition, the information about internal qualities that determine fruit shelf-life can aid packers in making decisions about how and where to distribute their blueberry fruit through the supply chain.

ACKNOWLEDGEMENTS

The authors would like to thank the China Scholarship Council Program (Grant No. 201506300125) for providing financial support for Mengyun Zhang to conduct her doctoral research in the Bio-Sensing and Instrumentation Laboratory at the University of Georgia. This work is supported by the USDA National Institute of Food and Agriculture (NIFA) Specialty Crop Research Initiative Program (Grant No. 2014-51181-22383). Mention of company or trade names is for description only and does not imply endorsement by the USDA. The USDA is an equal opportunity provider and employer.

Co-author Fuzeng Yang is financially supported by the National Key R&D Program of China "the 13th Five-Year Plan" (Program No. 2016YFD0700503), Major Program of Cooperative Innovation for Yangling Demonstration Zone (Program No. 2016CXY-20), and Shaanxi Provincial Agricultural Technology Program of Innovation and Development (Program No. 2016NY-127).

The authors gratefully thank Renee Allen (University of Georgia Area Extension Agent for Commercial Blueberry Production in Alma, Ga.) and Yu Jiang for providing critical suggestions and comments on the experimental design and data analysis, as well as the members of the Bio-Sensing and Instrumentation Laboratory at the University of Georgia (Jamal Hunter, Jesse Kuzy, Rui Xu, Lin Qi, and Shangpeng Sun) for their assistance in collecting blueberry samples and conducting the experiments.

REFERENCES

Almenar, E., Samsudin, H., Auras, R., Harte, B., & Rubino, M. (2008). Postharvest shelf life extension of blueberries using a biodegradable package. *Food Chem., 110*(1), 120-127. http://dx.doi.org/10.1016/j.foodchem.2008.01.066

Ariana, D. P., & Lu, R. (2008). Detection of internal defect in pickling cucumbers using hyperspectral transmittance imaging. *Trans. ASABE, 51*(2), 705-713. https://doi.org/10.13031/2013.24367

Baritelle, A. L., & Hyde, G. M. (2001). Commodity conditioning to reduce impact bruising. *Postharvest Biol. Tech., 21*(3), 331-339. http://dx.doi.org/10.1016/S0925-5214(00)00154-X

Brown, G. K., Schulte, N. L., Timm, E. J., Beaudry, R. M., Peterson, D. L., Hancock, J. F., & Takeda, F. (1996). Estimates of mechanization effects on fresh blueberry quality. *Appl. Eng. Agric., 12*(1), 21-26. https://doi.org/10.13031/2013.25435

Brown, G. K., Segerlind, L. J., & Summitt, R. (1974). Near-infrared reflectance of bruised apples. *Trans. ASAE, 17*(1), 17-19. https://doi.org/10.13031/2013.36775

Burda, S., Oleszek, W., & Lee, C. Y. (1990). Phenolic compounds and their changes in apples during maturation and cold storage. *J. Agric. Food Chem., 38*(4), 945-948. https://doi.org/10.1021/jf00094a006

Cheng, X., Chen, Y. R., Tao, Y., Wang, C. Y., Kim, M. S., & Lefcourt, A. M. (2004). A novel integrated PCA and FLD method on hyperspectral image feature extraction for cucumber chilling damage inspection. *Trans. ASAE, 47*(4), 1313-1320. https://doi.org/10.13031/2013.16565

Chiabrando, V., Giacalone, G., & Rolle, L. (2009). Mechanical behaviour and quality traits of highbush blueberry during postharvest storage. *J. Sci. Food Agric., 89*(6), 989-992. https://doi.org/10.1002/jsfa.3544

Clark, C. J., McGlone, V. A., & Jordan, R. B. (2003). Detection of brownheart in 'Braeburn' apple by transmission NIR spectroscopy. *Postharvest Biol. Tech., 28*(1), 87-96. http://dx.doi.org/10.1016/S0925-5214(02)00122-9

Clark, C. J., McGlone, V. A., De Silva, H. N., Manning, M. A., Burdon, J., & Mowat, A. D. (2004). Prediction of storage disorders of kiwifruit (*Actinidia chinensis*) based on visible-NIR spectral characteristics at harvest. *Postharvest Biol. Tech., 32*(2),

147-158. http://dx.doi.org/10.1016/j.postharvbio.2003.11.004
Dale, A., Hanson, E. J., Yarborough, D. E., McNicol, R. J., Stang, E. J., Brennan, R., ... Hergert, G. B. (1994). Mechanical harvesting of berry crops. In *Horticultural reviews* (Vol. 16, pp. 255-382). https://doi.org/10.1002/9780470650561.ch8
DeMartino, G., Massantini, R., Botondi, R., & Mencarelli, F. (2002). Temperature affects impact injury on apricot fruit. *Postharvest Biol. Tech., 25*(2), 145-149. http://dx.doi.org/10.1016/S0925-5214(01)00165-X
FAOSTAT. (2014). Crops production. Rome, Italy: United Nations FAO. Retrieved from http://www.fao.org/faostat/en/#data/QC
Goliáš, J., Bejček, L., Graetz, P., & Klusáček, S. (2003). Mechanical resonance method for evaluation of peach fruit firmness. *Hort. Sci. (Prague), 30*, 1-6.
Han, D., Tu, R., Lu, C., Liu, X., & Wen, Z. (2006). Nondestructive detection of brown core in the Chinese pear 'Yali' by transmission visible-NIR spectroscopy. *Food Control, 17*(8), 604-608. http://dx.doi.org/10.1016/j.foodcont.2005.03.006
Hu, M.-H., Dong, Q.-L., & Liu, B.-L. (2016). Classification and characterization of blueberry mechanical damage with time evolution using reflectance, transmittance, and interactance imaging spectroscopy. *Comput. Electron. Agric., 122*, 19-28. http://dx.doi.org/10.1016/j.compag.2016.01.015
Ito, H., Fukino-Ito, N., Horie, H., & Morimoto, S. (2003). Non-destructive detection of physiological disorders in melons using near-infrared (NIR) spectroscopy. *Acta Hort. 654,* 229-234. http://dx.doi.org/10.17660/ActaHortic.2004.654.25
Jackson, E. D., Sanford, K. A., Lawrence, R. A., McRae, K. B., & Stark, R. (1999). Lowbush blueberry quality changes in response to prepacking delays and holding temperatures. *Postharvest Biol. Tech., 15*(2), 117-126. http://dx.doi.org/10.1016/S0925-5214(98)00075-1
Jiang, Y., Li, C., & Takeda, F. (2016). Nondestructive detection and quantification of blueberry bruising using near-infrared (NIR) hyperspectral reflectance imaging. *Sci. Rep., 6*, article 35679. https://doi.org/10.1038/srep35679
Kawano, S., Fujiwara, T., & Iwamoto, M. (1993). Nondestructive determination of sugar content in satsuma mandarin using near-infrared (NIR) transmittance. *J. Japanese Soc. Hort. Sci., 62*(2), 465-470. https://doi.org/10.2503/jjshs.62.465
Lu, R., & Ariana, D. P. (2013). Detection of fruit fly infestation in pickling cucumbers using a hyperspectral reflectance/transmittance imaging system. *Postharvest Biol. Tech., 81*, 44-50. http://dx.doi.org/10.1016/j.postharvbio.2013.02.003
Lu, R., Cen, H., Huang, M., & Ariana, D. P. (2010). Spectral absorption and scattering properties of normal and bruised apple tissue. *Trans. ASABE, 53*(1), 263-269. https://doi.org/10.13031/2013.29491
Marlow, G. C., & Loescher, W. H. (1984). Watercore. In *Horticultural reviews* (Vol. 6, pp. 189-251). https://doi.org/10.1002/9781118060797.ch6
Mazza, G., Kay, C. D., Cottrell, T., & Holub, B. J. (2002). Absorption of anthocyanins from blueberries and serum antioxidant status in human subjects. *J. Agric. Food Chem., 50*(26), 7731-7737. https://doi.org/10.1021/jf020690l
Miller, A. R., Kelley, T. J., & White, B. D. (1995). Nondestructive evaluation of pickling cucumbers using visible-infrared light transmission. *J. American Soc. Hort. Sci., 120*(6), 1063-1068.
Mitsuhashi-Gonzalez, K., Pitts, M. J., Fellman, J. K., Curry, E. A., & Clary, C. D. (2010). Bruising profile of fresh apples associated with tissue type and structure. *Appl. Eng. Agric., 26*(3), 509-517. https://doi.org/10.13031/2013.29942
Miyamoto, K., & Kitano, Y. (1995). Non-destructive determination of sugar content in satsuma mandarin fruit by near-infrared transmittance spectroscopy. *J. Near Infrared Spectrosc., 3*(4), 227-237. https://doi.org/10.1255/jnirs.73
Nanos, G. D., Lazaridou, M., Tsoukidou, M., & Sfakiotakis, E. M. (1997). Effect of temperature and propylene on apricot ripening. *Acta Hort. 488*, 619-624. https://doi.org/10.17660/ActaHortic.1999.488.100
NASS. (2014). National statistics for blueberries. Washington, DC: USDA National Agricultural Statistics Service. Retrieved from https://quickstats.nass.usda.gov/results/27A32234-4C1E-332B-8199-B50611DFC5A8
Nunes, M. C. N., Emond, J.-P., & Brecht, J. K. (2004). Quality curves for highbush blueberries as a function of the storage temperature. *Small Fruits Rev., 3*(3-4), 423-440. https://doi.org/10.1300/J301v03n03_18
Opara, U. L., & Pathare, P. B. (2014). Bruise damage measurement and analysis of fresh horticultural produce: A review. *Postharvest Biol. Tech., 91*, 9-24. http://dx.doi.org/10.1016/j.postharvbio.2013.12.009
Prusky, D. (2011). Reduction of the incidence of postharvest quality losses, and future prospects. *Food Security, 3*(4), 463-474. https://doi.org/10.1007/s12571-011-0147-y
Qin, J., & Lu, R. (2005). Detection of pits in tart cherries by hyperspectral transmission imaging. *Trans. ASAE, 48*(5), 1963-1970. https://doi.org/10.13031/2013.19988
Schaare, P. N., & Fraser, D. G. (2000). Comparison of reflectance, interactance, and transmission modes of visible/near-infrared spectroscopy for measuring internal properties of kiwifruit (*Actinidia chinensis*). *Postharvest Biol. Tech., 20*(2), 175-184. http://dx.doi.org/10.1016/S0925-5214(00)00130-7
Schotte, S., De Belie, N., & De Baerdemaeker, J. (1999). Acoustic impulse-response technique for evaluation and modeling of firmness of tomato fruit. *Postharvest Biol. Tech., 17*(2), 105-115. http://dx.doi.org/10.1016/S0925-5214(99)00041-1
Slaughter, D., & Rohrbach, R. (1985). Developing a blueberry firmness standard. *Trans. ASAE, 28*(3), 986-992. https://doi.org/10.13031/2013.32374
Takeda, F., Krewer, G., Li, C., MacLean, D., & Olmstead, J. W. (2013). Techniques for increasing machine harvest efficiency in highbush blueberry. *HortTech., 23*(4), 430-436.
Tetteh, M. K. (2002). Measuring blueberry firmness and modeling quality changes for delays in cooling using the FirmTech II. PhD diss. Athens, GA: University of Georgia.
Toivonen, P. M. A., Hampson, C., Stan, S., McKenzie, D.-L., & Hocking, R. (2007). Factors affecting severity of bruises and degree of apparent bruise recovery in a yellow-skinned apple. *Postharvest Biol. Tech., 45*(2), 276-280. http://dx.doi.org/10.1016/j.postharvbio.2007.01.018
Upchurch, B. L., Throop, J. A., & Aneshansley, D. J. (1997). Detecting internal breakdown in apples using interactance measurements. *Postharvest Biol. Tech., 10*(1), 15-19. http://dx.doi.org/10.1016/S0925-5214(96)00057-9
Van linden, V., Scheerlinck, N., Desmet, M., & De Baerdemaeker, J. (2006). Factors that affect tomato bruise development as a result of mechanical impact. *Postharvest Biol. Tech., 42*(3), 260-270. http://dx.doi.org/10.1016/j.postharvbio.2006.07.001
Vogelmann, T. C. (1993). Plant tissue optics. *Annu. Rev. Plant Physiol. Plant Molecular Biol., 44*(1), 231-251. https://doi.org/10.1146/annurev.pp.44.060193.001311
Wang, W., Li, C., Tollner, E. W., Rains, G. C., & Gitaitis, R. D. (2012). A liquid crystal tunable filter based shortwave infrared spectral imaging system: Design and integration. *Comput. Electron. Agric., 80*, 126-134. http://dx.doi.org/10.1016/j.compag.2011.07.012
Xing, J., Jancsok, P., & De Baerdemaeker, J. (2007). Stem-end/calyx identification on apples using contour analysis in multispectral images. *Biosyst. Eng., 96*(2), 231-237. http://dx.doi.org/10.1016/j.biosystemseng.2006.10.018

Yu, P., Li, C., Takeda, F., & Krewer, G. (2014). Visual bruise assessment and analysis of mechanical impact measurement in southern highbush blueberries. *Appl. Eng. Agric., 30*(1), 29-37. https://doi.org/10.13031/aea.30.10224

Zhang, M., & Li, C. (2016). Blueberry bruise detection using hyperspectral transmittance imaging. ASABE Paper No. 162460707. St. Joseph, MI: ASABE. https://doi.org/10.13031/aim.20162460707